EUROGRAPHICS 2002 / G. Drettakis and H.-P. Seidel
(Guest Editors)

Volume 21 (2002), Number 2

Intrinsic Parameterizations of Surface Meshes

Mathieu Desbrun
USC

Mark Meyer
Caltech

Pierre Alliez
USC / INRIA

Abstract

Parameterization of discrete surfaces is a fundamental and widely-used operation in graphics, required, for instance, for texture mapping or remeshing. As 3D data becomes more and more detailed, there is an increased need for fast and robust techniques to automatically compute least-distorted parameterizations of large meshes. In this paper, we present new theoretical and practical results on the parameterization of triangulated surface patches. Given a few desirable properties such as rotation and translation invariance, we show that the only admissible parameterizations form a two-dimensional set and each parameterization in this set can be computed using a simple, sparse, linear system. Since these parameterizations minimize the distortion of different intrinsic measures of the original mesh, we call them Intrinsic Parameterizations. *In addition to this partial theoretical analysis, we propose robust, efficient and tunable tools to obtain least-distorted parameterizations automatically. In particular, we give details on a novel, fast technique to provide an optimal mapping without fixing the boundary positions, thus providing a unique* Natural Intrinsic Parameterization. *Other techniques based on this parameterization family, designed to ease the rapid design of parameterizations, are also proposed.*

1. Introduction

Parameterization is a central issue in graphics. Parameterizing a 3D mesh amounts to computing a correspondence between a discrete surface patch and an isomorphic planar mesh through a piecewise linear function or *mapping*. In practice, this piecewise linear mapping is simply defined by assigning each mesh node a pair of coordinates (u,v) referring to its position on the planar region. Such a one-to-one mapping provides a flat parametric space, allowing one to perform any complex operation directly on the flat domain rather than on the curved surface. This facilitates most forms of mesh processing, such as surface fitting, remeshing, or texture mapping. This last application, for instance, is widely used in Graphics as it dramatically enhances the visual richness of a 3D surface, both for overly simplified character meshes in game engines as well as for incredibly detailed complex surfaces in computer-generated feature films. Unfortunately despite numerous existing parameterization techniques [9, 23] and commercial applications (Maya, Softimage, Flesh), it usually takes several hours of tedious (u,v) adjustments for a talented user to map a texture correctly (i.e., with acceptable distortions) onto an arbitrary surface.

This failure can be partially blamed on the intrinsic difficulty of the problem at hand. Since we are basically trying to flatten a surface from 3D down to 2D, there is in general *no perfect way* to perform such a flattening without introducing some form of distortion. However, most existing techniques, supposed to minimize distortion, do not result in a visually "smooth parameterization", even more so for very irregular meshes issued from scanners as demonstrated in Figure 3.

The goal of this paper is to lay out a theoretical background on patch parameterization, as well as to develop a practical implementation. We will first define the notion of distortion measures between two 1-ring neighborhoods, exhibit the unique family of admissible distortion measures, derive from it a novel family of intrinsic parameterizations of surface patches, and propose fast algorithms to implement these theoretical results. We will also exhibit the practical results one can get at low cost using our novel technique, such as the boundary-free flattenings depicted in Figure 2.

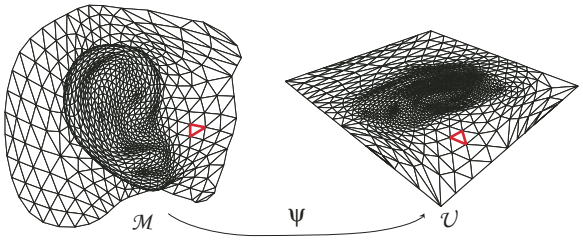

Figure 1: *A piecewise linear mapping between a 3D mesh M and an isomorphic flat mesh U, where a triangle on the mesh is mapped to a triangle in the parameterization.*

1.1. Problem Statement and Conventions

In this paper, we will deal with the following problem: *Given a piecewise linear mesh patch M, possibly with holes but non-closed, construct a piecewise linear mapping ψ between M and an isomorphic planar triangulation $U \in \mathbb{R}^2$ that best preserves the original, intrinsic characteristics of M.* Throughout the paper, we will denote by $\mathbf{x}_i$ the 3D position of the i^{th} node in the original mesh M, and by $\mathbf{u}_i$ the 2D position (parameter value) of the corresponding node in the 2D mesh U. We will also use the self-explanatory notation: $\mathbf{x}_i = (x_i, y_i, z_i)^t$, $\mathbf{u}_i = (u_i, v_i)^t$. Parameterizing a mesh is therefore providing the piecewise linear mapping ψ (see Figure 1)

such as:

$$\psi: \quad M \to U$$
$$\mathbf{x}_i \to \mathbf{u}_i$$

Texturing the mesh M will then be as simple as pasting a picture onto the parameter domain, and mapping each triangle of the original mesh M with the part of the picture present within the associated triangle in the parameter plane.

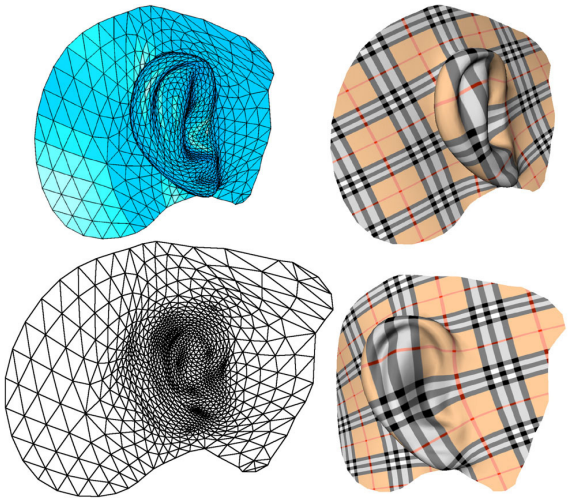

Figure 2: *Left: A 3D surface (top) and its natural conformal parameterization (bottom). Right: Views of the 3D surface.*

1.2. Background

Due to its primary importance for any subsequent mesh manipulation, the subject of mesh parameterization has been researched for a number of years, and not only in Computer Graphics.

Computer Graphics A significant body of work on parameterization has been published over the last ten years in Computer Graphics. Almost all techniques explicitly aim at producing least-distorted parameterizations, and vary only by the distortions considered and the minimization processes used. Early work used the notion of flattening to obtain an isomorphic planar triangulation [1, 26, 40], often minimizing discrete variables in the process, such as the ratio of angles between the 3D triangles and their associated 2D versions [3, 39, 4]. Others considered spring-like energies [20, 29, 2, 21, 9, 22, 31, 10, 25] that can be minimized quickly by a linear system solver when the boundary has been fixed to an arbitrary contour (with the noticeable exception of [23] where only a few internal points need to be fixed by the user).

The Discrete Conformal Parameterization (DCP) has been proposed independently by a number of authors [30, 7, 16] who derived the same linear condition for conformality either using Differential Geometry, harmonic maps, or Finite Elements. Here again, a boundary condition is needed to induce a conformal mapping.

Finally, one can use nonlinear formulations to define an optimal parameterization [17, 32]. The MIPS method for instance finds a "natural boundary" that minimizes their highly non-linear energy [17]. Unfortunately, this requires quite a computational effort (even if hierarchical solvers can be used [18, 35]) for a result visually very close to the DCP. Sander and co-authors [36] proposed yet another nonlinear energy for the specific problem of texture stretch distortion.

Most of these techniques proposed to minimize a continuous energy over a piecewise linear surface. However, the choice of the energy sometimes seems very arbitrary, and most of them may visually result in non-smooth parameterizations and therefore non-smooth textured meshes, as demonstrated in Figure 3(b-c). Note that using [36] results in a smooth parameterization, but takes more than six minutes to converge since it requires a non-linear minimization. In our experience, the only parameterizations that consistently provide visually smooth parameterizations are Floater's [9, 8].

Cartography Concurrently, cartographers have been dealing with the parameterization of non-flat surfaces for centuries, in order to represent our spherical earth as flat maps. Their work has mainly focused on differential parameterization, and is therefore only marginally relevant in Computer Graphics in practice. It is however interesting to mention that it is well known in this field that a mapping of a curved surface can either be *authalic* (i.e., area-preserving), or *conformal* (i.e., angle-preserving). No mapping of the earth can be *isometric* (i.e., distance-preserving): as it would have to be *both* authalic and conformal, and this is strictly impossible for non-developable surfaces like a sphere and most other geometries. This paper establishes similar results, but for discrete surfaces, extending the known continuous differential geometry results as well as providing insights for novel notions.

1.3. Overview

In this paper, we restrict ourselves to the parameterization of non-closed triangulated surfaces since many existing papers already describe different techniques to split a closed object into a series of patches (also called atlas of charts [14, 11, 36, 24]). We demonstrate that the set of desirable mappings for such patches form a simple low-dimensional space (Section 2). Moreover, the two generative parameterizations of this space are the existing discrete conformal mapping and a novel discrete authalic mapping, and all other valid *intrinsic* parameterizations can be found by simply solving a sparse linear system as detailed in Sections 3 and 4. We also demonstrate that they generate smooth texture mappings even for highly irregular meshes. We then show how easily one can find an optimal parameterization without fixing boundary points, providing a **natural** parameterization, by simply adding natural boundary conditions. Finally, we quickly review the possible immediate extensions that one could do with this new parameterization family before concluding.

2. Distortion Measures for 1-Rings

We want to preserve as much of the intrinsic qualities of a surface as we possibly can during its parameterization, i.e.,

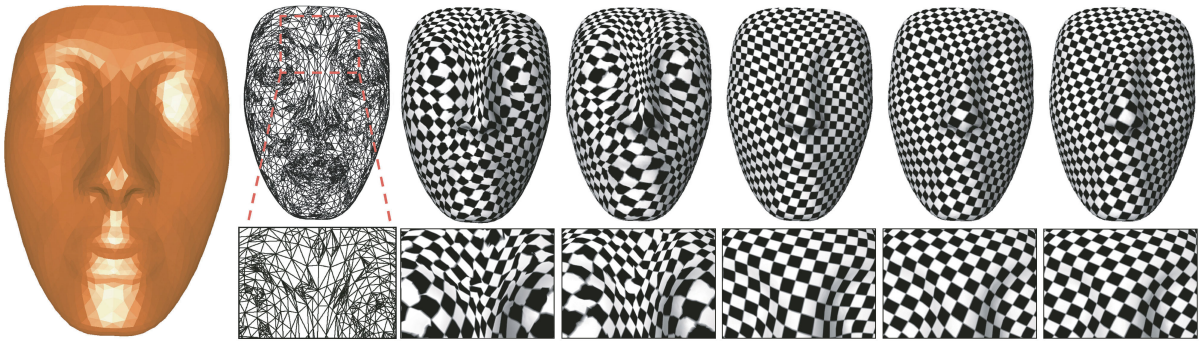

(a) irregular mesh (b) [41] (c) [20] (d) [36] (e) **DAP** (f) **DCP**

Figure 3: *Intrinsic Parameterizations: Most previous parameterization techniques (b-c) are not robust to mesh irregularity, exhibiting large distortions for highly irregular, yet geometrically smooth meshes such as in (a). Non-linear techniques (d) can achieve much better results, but often require several minutes of computational time. In comparison, with the exact same boundary conditions, our technique quickly generates very smooth parameterizations, regardless of the mesh irregularity (sampling quality) as demonstrated by the two texture-mapped members (e-f) of the novel parameterization family (denoted* Intrinsic Parameterizations*) that we introduce in this paper.*

its flattening. This implies that we need to first define what these intrinsic qualities are for a discrete surface: minimal distortion will then mean best preservation of these qualities. In this section, we restrict our investigation to the distortion measures between *simple 1-ring neighborhoods*, and demonstrate that the appropriate measures actually form a low dimensional space.

2.1. Notion of Distortion Measure

As in the problem statement, let M be a simple mesh embedded in 3D consisting of a 1-ring neighborhood (i.e., a vertex and all its adjacent triangles), and let U be an isomorphic mesh: $U \sim M$ (we use the symbol $\sim$ to indicate isomorphy). Figure 4 shows the mapping between two simple 1-ring neighborhoods. We define a *distortion measure* between M and U as a functional E taking two isomorphic triangulations as inputs, and returning a real value:

$$\begin{aligned} E: \quad & T \times T \rightarrow \mathbb{R} \\ & (M, U) \rightarrow E(M, U). \end{aligned}$$

This kind of functional is sometimes referred to as a *mutual energy*, as it can be seen as a measure of the energy required to distort one into the other. By the very definition of a distortion measure, $E(M, \cdot)$ must be minimum for M, as there is no mesh less distorted compared to M than itself.[†] We therefore have the following inequality for every U such that $U \sim M$:

$$E(M, M) \leq E(M, U) \tag{1}$$

For convenience, we will denote ϕ the distortion of a 1-ring with itself: $E(M, M) = \phi(M)$. Thus, ϕ is a *measure* (sometimes called *energy*) of the triangulated surface. In order to further investigate what the appropriate distortion measures are for 1-rings, we now explore what the possible measures of a mesh are, since it will restrict the possible set of distortion measures.

[†] Note however that there generally exist other meshes, different from M, that also achieve the same energy minimum.

2.2. Properties of Intrinsic Measures

A measure of a mesh is a *functional* ϕ which, given a piecewise-linear surface patch M, basically returns a "score" $\phi(M)$. This functional must satisfy a few *basic properties*, that we now go over.

- **Rotation and Translation Invariance** Obviously, we want the functional to be *invariant* to any translation or rotation of the mesh. Since these affine transformations do not affect the geometry of the mesh, the measure should remain identical. This will consequently render the parameterization independent of rotation and translation of the input mesh.
- **Continuity** We also want the functional to be a discrete version of a continuous measure, consistent with the continuous, differential case. Thus, the functional needs to converge to a continuous measure as we get a finer and finer triangulation, under some possible additional conditions (such as bounded fatness, or more generally, non-degenerated triangulations). This is called *conditional continuity*, and is usually stated as:

  $$\phi(M_n) \rightarrow \phi(M) \text{ if } M_n \rightarrow M \text{ as } n \rightarrow \infty.$$

  Here again, this will induce a very natural property for our parameterizations.
- **Additivity** A measure should also be *additive*, i.e.:

  $$\phi(M_1 \cup M_2) + \phi(M_1 \cap M_2) = \phi(M_1) + \phi(M_2).$$

  The measure with such a property has the desirable quality of being *intrinsic*, that is to say, it *only depends on the surface itself*, not on its sampling. To illustrate this fact, consider the addition of one or several vertices onto the existing surface (along the boundary or inside a triangle for instance); it is easy to verify that the functional will still return the same measurement, since the real geometry of the surface is not affected – only its discretization, hence the term intrinsic. This sampling-independent property will be particularly attractive when dealing with large

meshes, since hierarchical solvers will prove particularly efficient in solving for the parameterization.

2.3. Admissible Intrinsic Measures

Although the restrictions imposed on the notion of measure seem to be loose and natural, there are, surprisingly, only a small family of functionals that meet the requirements.

Minkowski Functionals of 2-Manifolds A set of well-known functionals satisfies all the previous conditions. These are called the Minkowski functionals. For 2D surfaces, there are three such functionals: the **Area** ϕ^A, the **Euler characteristic** ϕ^χ, and the **Perimeter** ϕ^P (length of the boundary) of a triangle mesh. It is straightforward to check that each of these functionals meet the three conditions we just listed. It is also interesting to notice that the two first ones (the perimeter being only a boundary measure) correspond respectively to the integrals of the determinants of the *first*— area element — and of the *second*— Gaussian curvature —*fundamental forms* [13]. These are well-known to be *intrinsic* in the differential geometry sense, meaning that they could be computed by "inhabitants" of the surface having no knowledge of the actual embedding of the surface.

Admissible Functionals Since we are looking for measures over a triangulation, a result dating back to the previous century explicitly states the set of all admissible functionals. A triangulation (considered as a 2-manifold, and disregarding its embedding) belongs to the *convex ring*, since it is the union of a set of triangles, therefore a union of convex bodies (which does *not* mean that the triangulation itself has to be convex). On this convex ring, Hadwiger [15] has proven that the only functionals, defined over the convex ring, matching the three conditions we mentioned above are *linear combinations of the Minkowski functionals* ‡. Therefore, the only admissible functionals fitting the three previous properties are *linear combinations of Area, Euler characteristic, and Perimeter*. The set of all admissible functionals is therefore a 3-dimensional space, and for any admissible measure ϕ, there exists a *unique* triplet of constants c_1, c_2, c_3 such that:

$$\phi = c_1\,\phi^A + c_2\,\phi^\chi + c_3\,\phi^P. \qquad (2)$$

Valid Distortion Measures Between 1-rings

Let's go back to our measures of distortion between two isomorphic 1-rings. Since the distortion measures must match the intrinsic measures, this restrains the admissible set to a special subset of the general case proven in [34], because of the additional additivity and continuity conditions. We show in the next section that the *simplest* relevant distortion measures form a two-dimensional space.

3. Optimal 1-Ring Flattening

We now introduce the only quadratic distortion measures that fit the requirements that we derived in the previous sections. We show that their critical points, when a boundary condition is imposed, can be found by solving a simple linear equation. We start by developing the two most representative optimal mappings, the *discrete conformal parameterization* (DCP) and the novel *discrete authalic parameterization* (DAP), and demonstrate how all the others can be deduced from their formulation. We also point to some of the similarities between the differential and the discrete case.

3.1. Notion of Optimal Vertex Placement

We call an *optimal 1-ring parameterization* any mapping from a given 3D 1-ring M to an isomorphic 2D 1-ring U that is the minimum of a distortion measure (as previously defined) for a fixed, given boundary mapping $\psi(\partial M)$. Therefore, if a distortion measure E is known and if each boundary vertex $\mathbf{x}_j$ has a given parameter value $\mathbf{u}_j$, the condition for the 2D 1-ring to be minimally distorted (i.e., optimal) is simply that $E(M, U)$ is minimum over all $U \sim M$, which yields this simple condition for the center node $\mathbf{u}_i$ of the 1-ring in the parameter plane:

$$\frac{\partial E}{\partial \mathbf{u}_i} = 0.$$

We shall now describe what the appropriate energies E are that define a distortion measure between two meshes. The first one is known under the name of Dirichlet energy.

3.2. Discrete Conformal Mapping

The first optimal mapping is actually already known. We now recall a bit of history and background to demonstrate the connection to our problem, and later build upon it.

Conformality on Differential Surfaces: While working on the area minimization problem introduced by the Belgian physicist Plateau, Mrs. Rado, Douglas, and later Courant proposed the use of the Dirichlet energy of a mapping instead of the highly nonlinear area functional previously used (see [30] for a good overview). The simple idea behind this functional [13] is that, in differential geometry, the area of a patch M is:

$$\begin{aligned} \text{Area} &= \tfrac{1}{2}\int_M |f_u \times f_v|\ du dv \le \tfrac{1}{2}\int_M\ |f_u|\,|f_v|\ du dv \\ &\le \tfrac{1}{4}\int_M (f_u^2 + f_v^2)\, du dv = \text{Dirichlet energy}. \end{aligned}$$

It is simple to verify that the first inequality becomes an equality iff $f_u \cdot f_v = 0$ everywhere, while the second does iff $|f_u| = |f_v|$ (deriving from the positivity of $(f_u - f_v)^2$). A further analysis [13] shows that the minimum of this energy (quadratic in the parameterization) is the area, and is only attained for *conformal mappings*, i.e., mappings where the two previously introduced conditions on f hold. Conformality of the map equivalently means *angle preservation* since these conditions imply that any angle between two vectors on the parameter plane will be preserved through the mapping. In other words, in the differential case, it is known that a conformal map will result from the minimization of the Dirichlet energy.

Dirichlet Energy on Triangulations: Pinkall and Polthier provided a formal derivation of the Dirichlet energy between two triangles in [30] for piecewise linear parameterizations. Summing the energies over the whole 1-ring, they found:

$$E_A = \sum_{\text{oriented edges}(i,j)} \cot\alpha_{ij}\,|\mathbf{u}_i - \mathbf{u}_j|^2, \qquad (3)$$

‡ Hadwiger's book has never been translated in English. There are however several books [37] and papers [38, 19] that clearly state the aforementioned theorem.

where $|\mathbf{u}_i - \mathbf{u}_j|$ is the length of the edge (i, j) in the parameter domain, and α_{ij} is the opposite left angle in 3D as shown in Figure 4. This nicely complements the differential case since this is also a quadratic energy in the parameterization, and that this discrete energy depends *only on the angles* of the original surface. Indeed, the only term depending on the original surface is the cotangent term. This energy is also equal, at its minimum, to the total surface area $\phi^A(M)$ when applied on the identity map (i.e., when $\mathbf{u}_{ij}$ is taken to be the actual 3D edge), and is therefore the exact equivalent of the Equation 1: E_A represents a distortion measure that fits our requirements defined in Section 2.

Critical Point of E_A: Mimicking the differential case, Pinkall and Polthier [30] proposed to define the *discrete conformal map* to be the critical point (a.k.a. the minimum) of the Dirichlet energy. Since this energy is quadratic, the derivation results in a simple linear system, that has a provably unique solution which is easy to compute once we fix the boundaries in the parameter domain. Notice that we can not formally claim this mapping to be angle-preserving, since there is generally no way to flatten a curved, discrete surface with a one-to-one correspondence of the 3D angles to the 2D angles. However, since the Dirichlet energy depends only on the 3D angles, and that in the differential case, the minimum of the Dirichlet energy is indeed conformal, this definition results in a visually satisfying parameterization as depicted in Figures 3(f) and 6(a). This explains the success (and the name) of this discrete conformal parameterization (DCP). Due to the simple formulation of this energy, deriving its critical point is rather simple, yielding the linear equation for the central node *i*:

$$\frac{\partial E_A}{\partial \mathbf{u}_i} = \sum_{j \in N(i)} (\cot \alpha_{ij} + \cot \beta_{ij}) (\mathbf{u}_i - \mathbf{u}_j) = 0. \qquad (4)$$

Again, we can note that the linear coefficients are functions of only the angles of the original surface. We will describe in detail the computations required to numerically solve for the parameterization in Section 4, as well as an extension to natural boundary conditions.

2D Analogy Consider a mesh vertex in flatland (2D) and its immediate neighboring vertices. Any motion of this vertex $\mathbf{u}_i$ in the plane will preserve the *1-ring area*, as mentioned in [5]. Therefore, computing the gradient of the 1-ring area with respect to $\mathbf{u}_i$ will provide a nontrivial equation (the gradient for each triangle being nonzero) that does always sum to zero (since the total area is constant). Not surprisingly, Appendix A shows that we find the same coefficients as in Equation 4. Indeed, ϕ^A is the area of mesh, and therefore, the coefficients of $\partial E_A(M, M)/\partial \mathbf{x}_i$ must match those of $\partial E_A(M, U)/\partial \mathbf{u}_i$ — giving an alternate, simple derivation of the conformality condition.

3.3. Discrete Authalic Mapping

Similarly to $E_A(M, \cdot)$ matching ϕ^A on the identity map of M, we now discuss the existence of a novel quadratic energy E_χ that matches the Euler characteristic χ on the identity map while being a valid distortion measure. Despite the relative simplicity of the optimality condition, we did not find any mention of it for the differential or the discrete case in the vast literature available. We will show, however, that this new condition has smoothness qualities similar to those of the conformality condition.

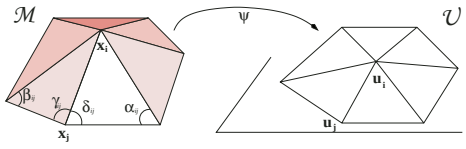

Figure 4: *A 3D 1-ring, and its associated flattened version.*

Hands-on Derivation Remember that the Euler characteristic is the integral of the Gaussian curvature. It is known [13, 27] that the Gaussian curvature, hence the determinant of the second fundamental form, is equal to $2\pi - \sum_j \theta_j$ where the θ_j's are the tip angles around $\mathbf{u}_i$. Therefore, a similar gradient computation can be done for the *sum of the tip angles* around $\mathbf{u}_i$. Indeed, for a flat triangulation, this sum also remains constant (and is equal to 2π) as $\mathbf{u}_i$ moves within the plane. This time, we get new coefficients as proven in Appendix B. From this simple derivation, we now derive an appropriate energy E_χ in the next paragraph.

Chi Energy on Triangulations Guided by the previous derivation, we introduce the following quadratic energy:

$$E_\chi = \sum_{j \in N(i)} \frac{(\cot \gamma_{ij} + \cot \delta_{ij})}{|\mathbf{x}_i - \mathbf{x}_j|^2} (\mathbf{u}_i - \mathbf{u}_j)^2 \qquad (5)$$

where the angles γ_{ij} and δ_{ij} are defined in Figure 4. This energy is constant for a given 1-ring when evaluated on the identity map, and therefore can always be scaled and shifted to be equal to χ (1 for a closed 1-ring). Additionally, since it is quadratic, we can show that it is greater than (or equal to) χ (after the above scaling and shifting) for any other map with the same boundary. This energy therefore satisfies all the properties we required in Section 2.

Critical Point of E_χ Once again, the optimal parameterization deriving from E_χ is easily obtained when the center node $\mathbf{u}_i$ satisfies:

$$\frac{\partial E_\chi}{\partial \mathbf{u}_i} = \sum_{j \in N(i)} \frac{(\cot \gamma_{ij} + \cot \delta_{ij})}{|\mathbf{x}_i - \mathbf{x}_j|^2} (\mathbf{u}_i - \mathbf{u}_j) = 0. \qquad (6)$$

Duality of E_A and E_χ Now, the coefficients of both this optimality condition and of E_χ are shown (also in the appendix) to be only functions of local areas of the 3D mesh. This should not come as a complete surprise: remember that the Dirichlet energy, which derives from the determinant of the first fundamental form, a measure of the local **area extension** [13], depends only on local **angles** and provides an **angle-preserving** mapping when minimized. Since χ is (up to a constant) the integral of the determinant of the second fundamental, which is a measure of the local **angle excess** [13],

we have a dual situation here. The energy E_χ is now depending only on local **areas**, and we therefore denote it *Discrete Authalic Parameterization* (DAP) for the same reasons as the DCP. Solving for the optimality of E_χ, using numerical methods described in Section 4, results in smooth parameterizations as shown on Figures 3(e) and 6(b). Just like the DCP does for the angles, the DAP tries to preserve the area structure of the original 1-ring.

3.4. General Discrete Parameterization

As mentioned in Section 3, the set of all admissible measures are linear combinations of the Minkowski functionals. For fixed boundary conditions, the only distortion measures possible are linear combinations of the area and the angle distortion measures (note: the perimeter distortion does not induce a particular position for the center vertex being a lower-order (1D) distortion measure for the boundary only). Therefore, it results that the family of admissible, simple distortion measures of a 1-ring is reduced to *linear combinations of the two discrete distortion measures* defined above. A general distortion measure E as we defined can thus always be written as:

$$E = \lambda E_A + \mu E_\chi$$

where λ and μ are two arbitrary real constants. The optimality condition will simply be a linear combination of the two optimality condition we have described above. We call this 2-dimensional space of optimal discretizations *Intrinsic Parameterizations*, since they naturally derive from intrinsic measures of the input mesh. As demonstrated in Figure 3, they provide smooth parameterizations even on highly irregular meshes since they minimize *intrinsic distortions*. Caveat: Although the DCP can easily be proven to be *globally* optimal (and therefore, angle-preserving when the triangulation is fine enough), the DAP is, as far as we know, only *locally* optimal. This means that we should not expect the DAP to perfectly preserve the area distortion across the mesh, but only as best as possible between each 1-ring.

3.5. Connection to Barycentric Coordinates

There exists a direct connection between barycentric coordinates and parameterization. It was already noted in [9, 12] that the coefficients of the usual linear systems used to parameterize meshes can be interpreted as barycentric coordinates of each internal vertex within its 1-ring. If the linear system for parameterization really represents barycentric coordinates, then *any flat mesh will be its own parameterization*, since each vertex will not move from its original position within its 1-ring. Although this condition seems to be an obvious quality for a "good" parameterization, only a few previous techniques satisfy this simple criterion. On the other hand, any linear combinations of the coefficients in Equations 4 and 6 defines perfectly valid barycentric coordinates [28]. We additionally proved that there is no other possible barycentric coordinates with the same properties, due to Hadwiger's theorem.

4. Parameterizing Meshes

We now discuss the practical implementation of the theoretical results presented above, along with convenient improvements to further aid in the design of good parameterizations. We first give details on how to solve for the least-distorted parameterizations with a fixed boundary, then show how to interactively move the boundaries to further reduce the burden of designing nice texture mapped surfaces, and finally present a natural parameterization that automatically finds an optimal boundary.

4.1. Computing an Intrinsic Parameterization

Since the gradients of the energies introduced in Section 3.4 are linear, computing a parameterization reduces to solving a sparse linear system:

$$\mathbf{MU} = \begin{bmatrix} \lambda\mathbf{M}^A + \mu\mathbf{M}^\chi & \\ \mathbf{0} & \mathbf{I} \end{bmatrix} \begin{bmatrix} \mathbf{U}^{\text{internal}} \\ \mathbf{U}^{\text{boundary}} \end{bmatrix} = \begin{bmatrix} \mathbf{0} \\ \mathbf{C}^{\text{boundary}} \end{bmatrix} = \mathbf{C}$$

where $\mathbf{U}$ is the vector of 2D-coordinates to solve for (separated for convenience into the internal vertices and the boundary vertices); $\mathbf{C}$ is a vector of boundary conditions that contains the positions where the boundary vertices are placed; and $\mathbf{M}^A$ and $\mathbf{M}^\chi$ are sparse matrices whose coefficients are given respectively by:

$$\mathbf{M}^A_{ij} = \begin{cases} \cot(\alpha_{ij}) + \cot(\beta_{ij}) & \text{if } j \in N(i) \\ -\sum_{k \in N(i)} \mathbf{M}^A_{ik} & \text{if } i = j \\ 0 & \text{otherwise,} \end{cases}$$

$$\mathbf{M}^\chi_{ij} = \begin{cases} \left(\cot(\gamma_{ij}) + \cot(\delta_{ij})\right) / |\mathbf{x}_i - \mathbf{x}_j|^2 & \text{if } j \in N(i) \\ -\sum_{k \in N(i)} \mathbf{M}^\chi_{ik} & \text{if } i = j \\ 0 & \text{otherwise.} \end{cases}$$

Note that this technique can handle an arbitrary number of boundary curves (they are simply additional boundary vertices) and therefore easily parameterize patches containing holes. Once the boundary points have been chosen (either automatically or by the user), the sparse system is efficiently solved using Conjugate Gradient with an appropriate preconditioning (we recommend SSOR or inverse diagonal preconditioning — see [33]).

Constraints The user may possibly want to constrain certain points to given parameter values. This can be easily achieved using Lagrange multipliers. Each point constraint creates a linear equation relating the parametric values of the vertices of the enclosing triangle (using triangular barycentric coordinates) to the constrained position. We then add these additional constraints to the linear system using standard Lagrange multipliers. The previous linear system is then augmented to the following system:

$$\begin{bmatrix} \mathbf{M} & (\mathbf{M}^\eta)^T \\ \mathbf{M}^\eta & \mathbf{0} \end{bmatrix} \begin{bmatrix} \mathbf{U} \\ \eta \end{bmatrix} = \begin{bmatrix} \mathbf{C} \\ \mathbf{C}^\eta \end{bmatrix}$$

where $\mathbf{M}^\eta_{ij}$ is 1 only if the j^{th} constraint constrains the i^{th} vertex and 0 otherwise, and $\mathbf{C}^\eta_j$ is set to the j^{th} constrained position. Note that constraining a line is also possible by simply constraining the endpoints as well as the intersections of the line with the edges of the mesh.

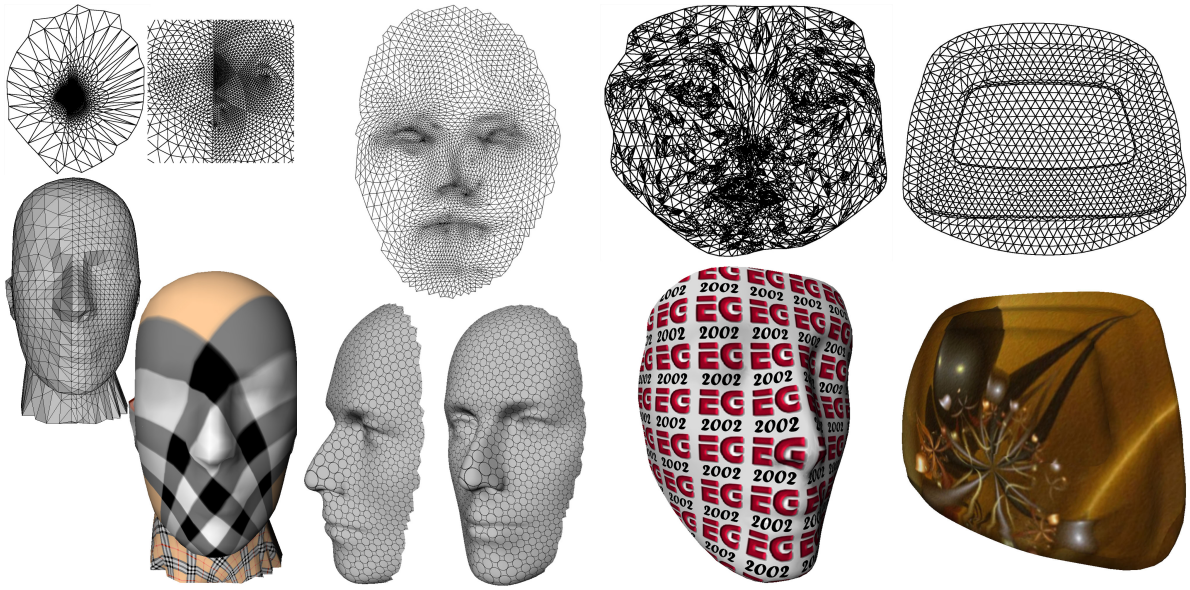

Figure 5: *Other Examples of Natural Conformal Maps: to demonstrate the conformality of the maps we obtain, we use an irregularly sampled mesh and observe that the symmetry is preserved despite the drastic change in sampling rate. The third natural parameterization uses the same mesh as in Figure 3. These four parameterizations were obtained in 0.8 s, 0.5 s, 1.8 s, and 0.3 s, respectively. See also color section.*

4.2. Modifying Boundaries

In addition to simple fixed-boundary conditions, we can allow the user to interactively modify the positions of boundary points while updating the parameterization in *realtime*. This efficiency is achieved by taking advantage of the linear nature of our solution and precomputing how the parameterization responds to the movement of a boundary point.

Impulse response We first precompute the parameterizations that result from placing one boundary point at $(1,1)$ and all others at $(0,0)$ (these correspond to the Green functions of our parameterization equation):

$$\mathbf{M}\mathbf{b}^i = \mathbf{e}^i, \quad \forall i \in \text{boundary}$$

where $\mathbf{e}^i$ is a 1D vector (i.e., a vector of scalars) containing 1 in i^{th} position and 0 elsewhere, while $\mathbf{b}^i$ is the unknown 1D vector.

Realtime Boundary Manipulation By solving this system once for every boundary point, we construct a set of "basis parameterizations" that describe how the parameterization is altered by a change in a single boundary position. Indeed, the parameterization can then be efficiently updated as the user manipulates the boundary by noting that:

$$\mathbf{C} = \left[\sum_{i \in \text{boundary}} (\mathbf{u}_i^{\text{boundary}})^T \mathbf{e}^i \right] = \mathbf{M} \left[\sum_{i \in \text{boundary}} (\mathbf{u}_i^{\text{boundary}})^T \mathbf{b}^i \right]$$

where $\mathbf{u}_i^{\text{boundary}}$ is the position of i^{th} boundary point. Therefore, the parameterization for a given set of boundary points can easily be reconstructed in realtime, allowing realtime boundary manipulation, as:

$$\mathbf{U} = \sum_{i \in \text{boundary}} (\mathbf{u}_i^{\text{boundary}})^T \mathbf{b}^i.$$

This novel feature provides an easy tool for a user to optimize the design of a texture mapping on arbitrary surface patches.

Natural Boundaries / Natural Conformal Map

Interestingly, we can also solve a similar linear system while letting the computer pick the "best" boundaries. Earlier, we showed how to get a parameterization once a boundary was given, but we can also solve for an optimal conformal mapping by imposing *natural boundaries* (also called Neumann boundaries). This requires only minor modifications to the prior algorithm, and due to the quadratic nature of the energy, we will also obtain a unique solution. As demonstrated in Appendix A, we show that the derivative of the Dirichlet energy on a triangle with respect to one of its vertices is equal to the opposite edge rotated by 90 degrees (such that $(x,y) \rightarrow (-y,x)$). A natural boundary condition is therefore to have the same property at the boundary. Summing over all adjacent triangles, the equation for the boundary point i (which we place into the matrix $\mathbf{M}$) becomes:

$$\sum_{\Delta_{ijk}} \cot\alpha(\mathbf{u}_i - \mathbf{u}_j) + \cot\beta(\mathbf{u}_i - \mathbf{u}_k) = \sum_{\Delta_{ijk}} R^{90}(\mathbf{u}_k - \mathbf{u}_j) \quad (7)$$

Where α and β are the angles at k and j, and R^{90} is a rotation by 90°. Note that this property also holds for interior vertices as the terms on the left become the conformal condition (Equation 4) and the terms on the right sum to zero.

To complete the minimization, we need to constrain two vertices to fix the rotation and translation of the resulting minimum parameterization. In our implementation, we constrain the two boundary vertices the farthest from each other to two arbitrary positions in the parameterization plane. This

simple modification results in *Natural Conformal Maps*, such as those depicted on Figures 2 and 5. Notice that these parameterizations take the same amount of time to compute as the fixed-boundary ones, offering a very nice tool for initial flattening before minor editing of the boundaries if necessary. Note also that if the authalic coefficients are proven, in the future, to derive from a global energy, a similar treatment can be used to find natural boundaries.

5. Nonlinear Optimization of Maps

The theoretical and practical work introduced in this paper opens many avenues. Aside from the natural conformal map and the entire family of intrinsic parameterizations by varying the parameters λ and μ, we can also compute parameterizations sufficiently close to these optimal ones to be visually smooth, but potentially more appropriate for a given application. Therefore, we propose two simple algorithms to compute good parameterizations that minimize other types of functionals.

5.1. Near-Optimal Maps

We sometimes wish to minimize highly nonlinear energies while remaining within the space of the aforementioned intrinsic parameterizations. In order to make this tractable, we can linearize the solution space by assuming that all solutions can be expressed as a linear combination of the two base intrinsic parameterizations:

$$\mathbf{U} = \lambda \mathbf{U}^A + (1-\lambda)\mathbf{U}^\chi. \tag{8}$$

Note that $\mu = 1-\lambda$ to ensure that the solution always interpolates the same boundary as we vary λ. Since we restrained the vector space of solutions to only linear combinations of the intrinsic parameterizations, many nonlinear functionals can be minimized by a simple low-order polynomial minimization (often in real time). Below are two simple examples of such functionals.

Edge-Length Distortion Minimization is achieved by minimizing the nonlinear energy:

$$E = \sum_{ij \in \text{Edges}} \left(\frac{|\mathbf{u}_i - \mathbf{u}_j|^2}{|\mathbf{x}_i - \mathbf{x}_j|^2} - 1\right)^2.$$

By substituting the values for $\mathbf{u}_i$ and $\mathbf{u}_j$ from equation 8, the energy becomes a quartic polynomial in λ. This energy can then be minimized in real time using a 3^{rd} order polynomial root finder to solve for: $\frac{dE}{d\lambda} = \sum_{ij \in \text{Edges}} 4\left(\frac{|\mathbf{u}_i - \mathbf{u}_j|^2}{|\mathbf{x}_i - \mathbf{x}_j|^2} - 1\right) \frac{(\mathbf{u}_i - \mathbf{u}_j)\cdot[(\mathbf{u}_i^A - \mathbf{u}_i^\chi) - (\mathbf{u}_j^A - \mathbf{u}_j^\chi)]}{|\mathbf{x}_i - \mathbf{x}_j|^2} = 0.$

Area Distortion Minimization can be achieved by minimizing: $E = \sum_{ijk \in \text{Faces}} \left(\left(\frac{A_{ijk}^{\text{param}}}{A_{ijk}^{\text{3D}}}\right)^2 - 1\right)^2$. As in the edge length distortion minimization, this results in a quartic polynomial in lambda and can be efficiently solved using a simple root finder. An example resulting from this technique is depicted in Figure 6

5.2. Boundary Optimization

Similar to the way we minimized an energy by modifying λ, we can, alternatively, minimize the energy by modifying the boundary of the parameterization. We first choose an appropriate energy (edge length distortion, area distortion, etc.), and then take its derivative with respect to each of the boundary points. Note that the terms of the form $\partial \mathbf{u}_i / \partial \mathbf{u}_p^{\text{boundary}}$ can be (pre)computed using the impulse response technique described in section 4.2. These derivatives are then used to perform a gradient descent to find a local minimum of the specified energy. Since the gradient descent is performed in terms of boundary points only (much fewer than the total number of points), this process is very efficient, and takes generally less than 10 seconds for several hundreds boundary vertices. A sequence of boundary optimizations using this method is depicted in Figure 7.

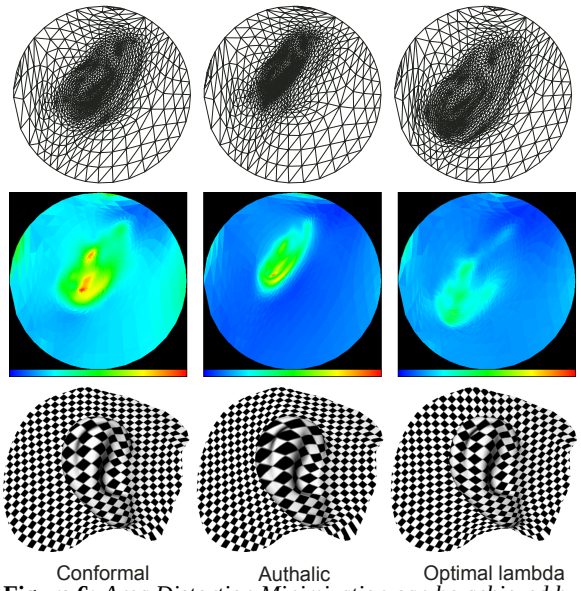

Figure 6: *Area Distortion Minimization can be achieved by optimizing the linear combination $\lambda \mathbf{U}^A + (1-\lambda)\mathbf{U}^\chi$ of the conformal and authalic parameterizations. The parameterizations (top) and the area distortion pseudo-coloring (middle) demonstrate the quality of the optimization (see color section).*

6. Results and Conclusions

All the results we obtained were computed in less than 5 seconds for fixed-boundary and natural parameterizations, and less than 15 seconds for boundary-optimized maps. These techniques are thus very well suited for interactive parameterization design. In summary, we have introduced the novel family of Intrinsic Parameterizations. We showed that they are the only parameterizations satisfying the proper conditions to make them easy to compute and robust to arbitrary meshes with guaranteed smoothness quality. We have also proposed algorithms to exploit these parameterizations and automatically design optimal maps, with or without boundary conditions. However, many other extensions can be thought of. Using least-squares as in [25], one could define other parameterizations very easily, based on the two main sets of coefficients introduced in this paper. Basically, any parameterization obtained by a linear system close to the co-

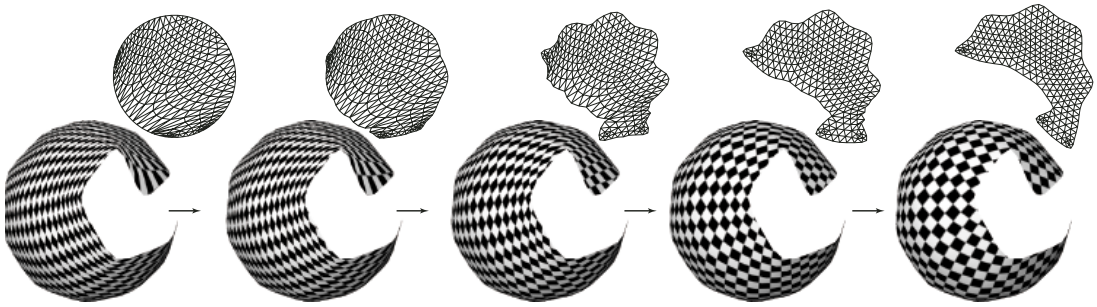

Figure 7: *Boundary Optimization: after choosing a (non)linear functional to minimize over the parameterization, we can move the boundary points to perform a gradient descent and optimize the parameterization. Here, an initial irregular spherical strip is mapped to a circle, then evolves towards an optimized parameterization (1.5 s) minimizing edge-length distortion.*

efficients of our Intrinsic Parameterizations will be visually smooth, providing us with a great deal of freedom to build other algorithms for parameterizations if more complex constraints must be enforced.

Independently, Levy [24] has developed an alternate derivation of the *Natural Conformal Maps*, in which he proves that the parameterization will not contain any folds (overlapping triangles). Therefore, future work may show that the *Natural Conformal Maps* are a discrete analog of the "Riemann Mapping Theorem".

Additional future work will focus on clarifying the relationship between our results and the existing body of work in Circle Packing, a technique which also provides the same kind of discrete mapping, but at the cost of a computationally expensive iterative process. Developing a good hierarchical solver as in [6] and in [35] could also speed up the process, making parameterization of extremely large meshes tractable. Finding optimal charts on a closed surface to locally parameterize a whole geometry is also of interest.

Acknowledgements The authors are extremely grateful to Martin Rumpf for his insightful comments. Thanks to David Cohen-Steiner for pointing us to Hadwiger's work, to Peter Schröder for support and instant German translation, to Jerrold Marsden, Anil Hirani and Andrei Khodakovsky for math support, to Tony DeRose for interesting discussions, to Isaac Cohen for pointers on differential geometry, and to the reviewers for extremely insightful comments. We also greatly benefited from a discussion with the authors of [36]. The work reported here was supported in part by IMSC, an NSF Engineering Research Center (EEC-9529152), and a NSF CAREER award (CCR-0133983).

References

1. BENNIS, C., VÉZIEN, J.-M., IGLÉSIAS, G., AND GAGALOWICZ, A. Piecewise Surface Flattening for Non-Distorted Texture Mapping. *Computer Graphics (Proceedings of SIGGRAPH 91) 25*, 4 (July 1991), pp.237–246.
2. CAMPAGNA, S., AND SEIDEL, H.-P. Parameterizing Meshes with Arbitrary Topology. In *Image and Multidimensional Digital Signal Processing* (1998), B. G. H. Niemann, H.-P. Seidel, Ed., pp.287–290.
3. C.L.WANG, C., CHEN, S.-F., FAN, J., AND M.F.YUEN, M. Two-dimensional Trimmed Surface Development using a Physics-based Model. *Proceedings of the 25th Design Automation Conference* (Sept. 1999). Paper No. DETC99/DAC-8634.
4. C.L.WANG, C., CHEN, S.-F., AND M.F.YUEN, M. Surface Flattening based on Energy Model. *Computer Aided Design* (*to appear*).
5. DESBRUN, M., MEYER, M., SCHRÖDER, P., AND BARR, A. H. Implicit Fairing of Arbitrary Meshes using Diffusion and Curvature Flow. In *Proceedings of SIGGRAPH 1999* (1999), pp.317–324.
6. DUCHAMP, T., CERTIAN, A., DEROSE, T., AND STUETZLE, W. Hierarchical Computation of PL Harmonic Embeddings". *Technical Report* (July 1997).
7. ECK, M., DEROSE, T., DUCHAMP, T., HOPPE, H., LOUNSBERY, M., AND STUETZLE, W. Multiresolution Analysis of Arbitrary Meshes. *Proceedings of SIGGRAPH 95* (August 1995), pp.173–182.
8. FLOATER, M. Mean Value Coordinates. *Preprint* (2002).
9. FLOATER, M. S. Parametrization and Smooth Approximation of Surface Triangulations. *Computer Aided Geometric Design 14*, 3 (1997), pp.231–250. ISSN 0167-8396.
10. FLOATER, M. S., AND REIMERS, M. Meshless parameterization and surface reconstruction. *Computer Aided Geometric Design 18*, 2 (March 2001), pp.77–92.
11. GARLAND, M., WILLMOTT, A., AND HECKBERT, P. S. Hierarchical Face Clustering on Polygonal Meshes. *2001 ACM Symposium on Interactive 3D Graphics* (March 2001), pp.49–58.
12. GOTSMAN, C., AND SURAHHSKY, V. Guaranteed Intersection-free Polygon Morphing. *Computer and Graphics 25*, 1 (2001), pp.67–75.
13. GRAY, A., Ed. *Modern Differential Geometry of Curves and Surfaces.* Second edition. CRC Press, 1998.
14. GRIMM, C. M., AND HUGHES, J. F. Modeling Surfaces of Arbitrary Topology using Manifolds. *Proceedings of SIGGRAPH 95* (August 1995), pp.359–368.
15. HADWIGER, H. *Vorlesungen Über Inhalt, Oberfläche und Isoperimetrie*. Springer-Verlag, 1957.
16. HAKER, S., ANGENENT, S., TANNENBAUM, A., KIKINIS, R., SAPIRO, G., AND HALLE, M. Conformal Surface Parameterization for Texture Mapping. *IEEE Transactions on Visualization and Computer Graphics 6*, 2 (April-June 2000), pp.181–189.
17. HORMANN, K., AND GREINER, G. MIPS: An Efficient Global Parametrization Method. In *Curve and Surface Design: Saint-Malo 1999* (2000), P.-J. Laurent, P. Sablonnière, and L. L. Schumaker, Eds., Vanderbilt University Press, pp.153–162.
18. HORMANN, K., GREINER, G., AND CAMPAGNA, S. Hierarchical Parametrization of Triangulated Surfaces. In *Proceedings of Vision, Modeling and Visualization* (1998), H.-P. S. B. Girod, H. Niemann, Ed., pp.219–226.

19. K. MICHIELSEN, H. DE RAEDT, J. F. Morphological Characterization of Spatial Patterns. *Prog. Theor/ Phys. Suppl. 138* (2000), pp.453–548.
20. KENT, J. R., CARLSON, W. E., AND PARENT, R. E. Shape Transformation for Polyhedral Objects. *Proceedings of SIGGRAPH 92* (July 1992), pp.47–54.
21. KRISHNAMURTHY, V., AND LEVOY, M. Fitting Smooth Surfaces to Dense Polygon Meshes. *Proceedings of SIGGRAPH 96* (August 1996), pp.313–324.
22. LEE, A. W. F., SWELDENS, W., SCHRÖDER, P., COWSAR, L., AND DOBKIN, D. MAPS: Multiresolution Adaptive Parameterization of Surfaces. *Proceedings of SIGGRAPH 98* (July 1998), pp.95–104.
23. LÉVY, B. Constrained Texture Mapping for Polygonal Meshes. *Proceedings of SIGGRAPH 2001* (August 2001), pp.417–424.
24. LÉVY, B., AND MAILLOT, J. Least Squares Conformal Maps for Automatic Texture Atlas Generation. *ACM SIGGRAPH Proceedings* (July 2002).
25. LÉVY, B., AND MALLET, J.-L. Non-Distorted Texture Mapping for Sheared Triangulated Meshes. *Proceedings of SIGGRAPH 98* (July 1998), pp.343–352.
26. MAILLOT, J., YAHIA, H., AND VERROUST, A. Interactive Texture Mapping. *Proceedings of SIGGRAPH 93* (August 1993), pp.27–34.
27. MEYER, M., DESBRUN, M., SCHRÖDER, P., AND BARR, A. H. Discrete Differential-Geometry Operators for Triangulated 2-Manifolds, 2002. submitted, found at http://www.multires.caltech.edu/pubs/difGeoOps.pdf.
28. MEYER, M., LEE, H., BARR, A. H., AND DESBRUN, M. Generalyzed Barycentric Coordinates for Irregular N-gons. *Journal Of Graphic Tools (to appear)* (2002).
29. PARIDA, L., AND MUDUR, S. Constraint-satisfying Planar Development of Complex Surfaces. *Computer Aided Design 25*, 4 (April 1993), pp.225–232.
30. PINKALL, U., AND POLTHIER, K. Computing Discrete Minimal Surfaces. *Experimental Mathematics 2*, 1 (1993), pp.15–36.
31. PRAUN, E., FINKELSTEIN, A., AND HOPPE, H. Lapped Textures. *Proceedings of SIGGRAPH 2000* (July 2000), pp.465–470.
32. PRAUN, E., SWELDENS, W., AND SCHRÖDER, P. Consistent Mesh Parameterizations. *Proceedings of SIGGRAPH 2001* (August 2001), pp.179–184.
33. PRESS, W., FLANNERY, B., TEUKOLSKY, S., AND VETTERLING, W. *Numerical Recipes in C: the Art of Scientific Computing*, 2nd ed. Cambridge University Press, 1994.
34. RUMPF, M. A Variational Approach to Optimal Meshes. *Numer. Math.*, 72 (1996), pp.523–540.
35. SANDER, P., GORTLER, S., SNYDER, J., AND HOPPE, H. Signal-Specialized Parameterization. *MSR Technical Report MSR-TR-2002-27* (2002).
36. SANDER, P. V., SNYDER, J., GORTLER, S. J., AND HOPPE, H. Texture Mapping Progressive Meshes. *Proceedings of SIGGRAPH 2001* (August 2001), pp.409–416.
37. SANTALO, L. A. *Integral Geometry and Geometric Probability*. Addison-Wesley, 1976.
38. SCHMALZING, J., AND KERSCHER, M. Minkowsky Functionals in Cosmology. *Generation of Large-Scale Structure in Cosmology* (1997), pp.255–260.
39. SHEFFER, A., AND DE STRULER, E. Surface Parameterization For Meshing by Triangulation Flattening. In *Proceedings of the 9th International Meshing Roundtable, Sandia National Laboratories* (Oct. 2000), pp.161–172.
40. SUN, M., AND FIUME, E. A Technique for Constructing Developable Surfaces. *Graphics Interface '96* (May 1996), pp.176–185.
41. TUTTE, W. T. How To Draw A Graph. *Proc. London Math. Soc.*, 13 (1963), pp.743–768.

Appendix A: Gradient of Area

A proof of the gradient of a triangle area with respect to a vertex, valid for an arbitrary embedding, can be found in [5]. It was proven that for a triangle (P,A,B) we get:

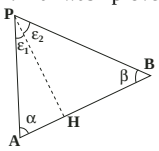

$$\nabla A = \frac{1}{2}\left((cot\ \beta)\ \mathbf{AP} + (cot\ \alpha)\ \mathbf{BP}\right)$$

where ∇ denotes the gradient with respect to $\mathbf{P}$. Additionally, since the area is equal to $|AB|$ times the height $|PH|$, we have another simple expression for the gradient (where "$\perp$" indicates a 90 degrees counter-clockwise rotation about the triangle's normal):

$$\nabla A = |AB|\nabla(|PH|) = |AB|\frac{\mathbf{PH}}{|PH|} = \mathbf{AB}^{\perp}.$$

Appendix B: Gradient of Angle

Despite an extensive literature search, we have not found any published derivation for the gradient of one of a triangle's angles with respect to its associated vertex. We therefore describe our derivation here.

Let $T = (P,A,B)$ be a triangle, and let H be the orthogonal projection of P onto the segment AB. We denote by ε_1 the angle $\widehat{APH}$, ε_2 the angle $\widehat{HPB}$, and ε the angle of T at P. Finally, we denote by α the angle at A and β the angle at B.

The gradient of ε with respect to $\mathbf{P}$ can be decomposed into the sum of the gradients of ε_1 and ε_2. Using the relation $cos(\varepsilon_1) = |PH|/|PA|$, the gradient can be computed as:

$$\nabla\varepsilon_1 = \nabla \arccos(|PH|/|PA|) = -\frac{|PA|}{|AH|}\nabla\left(\frac{|PH|}{|PA|}\right) \quad (9)$$

$$= -\frac{|PA|}{|AH|}\,\frac{\nabla(|PH|)\,|PA| - \nabla(|PA|)\,|PH|}{|PA|^2} \quad (10)$$

From the following identities: $\nabla|PA| = \mathbf{AP}/|PA|$, $\nabla|PH| = \mathbf{HP}/|PH|$, $\mathbf{HP} = \mathbf{HA} + \mathbf{AP}$, and $\cot\alpha = |AH|/|PH|$, we obtain:

$$\begin{aligned}\nabla\varepsilon_1 &= -\frac{|PA|}{|AH|}\left[\frac{\mathbf{HP}}{|PA|\,|PH|} - \frac{|PH|}{|PA|^3}\mathbf{AP}\right] \\ &= \frac{\mathbf{PA}}{|PA|^2}\left(\frac{|PA|^2}{|AH|\,|PH|} - \frac{|PH|}{|AH|}\right) + \frac{\mathbf{AH}}{|PH|\,|AH|} \\ &= \frac{\cot\alpha}{|PA|^2}\,\mathbf{PA} + \frac{\mathbf{AB}}{|PH|\,|AB|} \quad (11)\end{aligned}$$

The gradient of ε_2 will cancel out the last term, leading to the simple formula:

$$\nabla\varepsilon = \frac{\cot\alpha}{|PA|^2}\,\mathbf{PA} + \frac{\cot\beta}{|PB|^2}\,\mathbf{PB}$$

Notice that the vector weights can be expressed only in terms of local areas: if K is the orthogonal projection of B onto PA, then $\cot\alpha/|PA|^2$ is equal to the area of the triangle (A,B,K) divided by twice the square of the total area of triangle T.

Summing the contribution due to each triangle of a 1-ring, we obtain, with θ the total angle around $\mathbf{x}_i$ (in the notation of figure 4):

$$\nabla\theta = \sum_{j\in N_1(i)} \frac{(\cot\gamma_{ij} + \cot\delta_{ij})}{||\mathbf{x}_i - \mathbf{x}_j||^2}\,(\mathbf{x}_j - \mathbf{x}_i).$$